HYDRODYNAMIC MODELING OF OXIDIZER-RICH STAGED COMBUSTION INJECTOR FLOW*

J.V. Canino, S.D. Heister, and L.A. Garrison
School of Aeronautics and Astronautics
Purdue University
West Lafayette, IN

ABSTRACT

The main objective of this work is to determine the unsteady hydrodynamic characteristics of coaxial swirl atomizers of interest in oxidizer-rich staged combustion (ORSC) liquid rocket engines. To this end, the pseudo-density (homogeneous flow) treatment combined with the Marker-and-Cell (MAC) numerical algorithm has been used to develop an axisymmetric with swirl, two-phase, unsteady model. The numerical model is capable of assessing the time-dependent orifice exit conditions and internal mixing for arbitrary fuel and oxidizer gas injection conditions. Parametric studies have been conducted to determine the effect of geometry, gas properties, and liquid properties on the exit massflow rate and velocity. It has been found that the frequency at which the liquid film oscillates increases as the density ratio and collar thickness increase, decreases as film thickness and liquid swirl velocity increase, and is unaffected by the mixing length. Additionally, it has been determined that the variation in the massflow rate increases as the liquid swirl velocity and liquid film thickness increase, and decreases as the density ratio, collar thickness, and mixing length increase.

INTRODUCTION

Currently, there is interest in gaining a greater understanding into injectors that have application to oxidizer rich staged combustion (ORSC) engine cycles. These advanced cycles have application to liquid oxygen (LOX)/kerosene engines for use in launch vehicles and other applications. Russian engines, such as the RD-170 and RD-180 derivatives used on the Atlas V launch vehicle, have been developed based on this propellant combination, successfully operating at chamber pressures in excess of 2000 psi.

Figure 1 highlights within it the general features of the injector design that is used in the main combustion chamber of an ORSC engine. Many of the design features are intended to minimize tendency of the injector to participate in combustion instabilities as this issue is one of the most critical concerns for LOX/hydrocarbon engines. Oxidizer rich gas flows from the preburner into the central tube. An inlet lip may or may not be used at the entry point to affect the acoustic admittance into the preburner and feed system. In addition, the length of the gas channel can be varied to change the harmonic frequencies within the gas path in this region.

The kerosene/RP-1 is injected in the aft portion of the device and is swirled. While one may envision very poor mixing resulting from the swirling of the outer liquid flow, the bulk of the momentum in the system lies in the gas phase, and an ejector effect and fluid interface Kelvin-Helmholtz instabilities contribute to rapid mixing of the two propellant streams. The "mixing length" measured from the entry of the fuel to the injector face is a critical parameter in defining the injector geometry. Lengthening this distance improves mixing, but may result in film dryout within the injector and possible overheating from the local combustion zone. The submergence of the mixing region is believed to lead to an anchoring of the flame upstream of the injector face thereby reducing sensitivity to transverse oscillations within the combustion chamber. The height of the lip formed at the gas/liquid mixing interface is another geometric parameter of interest to designers.

Approved for public release; distribution is unlimited

* This work was accomplished under NASA Space Act Agreement NCC8-200

A computational model has been developed to provide an unsteady, axisymmetric, swirling flow solution to the laminar Navier-Stokes equations for this two-phase flow. The two-phase treatment is handled using the homogeneous flow approach in which a fictitious pseudo-density is introduced.

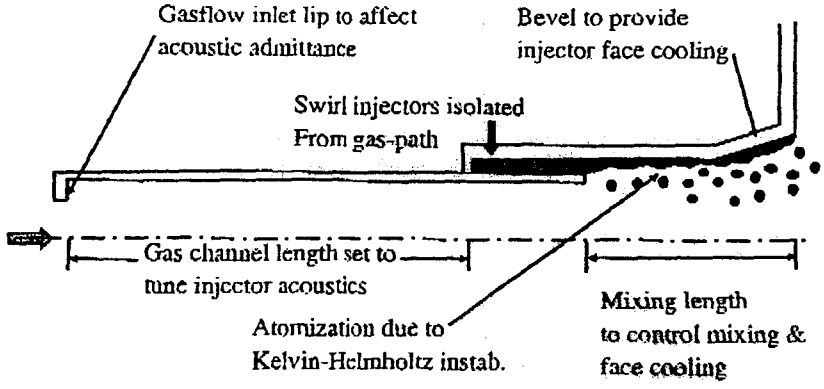

Figure 1. Schematic and General Features of ORSC Main Combustion Chamber Injector

The pseudo-density is varied between the gas and liquid density extremes; its evolution in time is computed via a constitutive relation developed by Kim, et. al.[1] Simulations are presented for various conditions to assess the influence of gas/liquid density ratio, mixing length, step height, and liquid swirl velocity over a range of conditions. The model is briefly described in the next section, followed by results and conclusions from the studies.

COMPUTATIONAL MODEL

The current 2D axisymmetric with swirl code utilizes the pseudo-density homogeneous fluid model. For the pseudo-density model, a nondimensional density is defined as the ratio of the density in a computational cell to the liquid density. Defining this pseudo-density allows the computation of the two phase flow using a single Navier-Stokes equation solver.

A finite volume formulation of the Marker-and-Cell method is used to solve the incompressible axisymmetric with swirl Navier-Stokes equations. Using the pseudo-density assumption, the Navier-Stokes equations reduce to Equations 1 through 4, shown below.

$$\frac{\partial(r\rho)}{\partial t}+\frac{\partial(r\rho v)}{\partial r}+\frac{\partial(r\rho u)}{\partial z}=0 \tag{1}$$

$$\frac{\partial(r\rho u)}{\partial t}+\frac{\partial(r\rho uv)}{\partial r}+\frac{\partial(r\rho uu)}{\partial z}=-r\frac{\partial P}{\partial z}+\frac{\partial}{\partial r}\left(\frac{1}{\mathrm{Re}^*}\frac{\partial(ru)}{\partial r}\right)+\frac{\partial}{\partial z}\left(\frac{1}{\mathrm{Re}^*}\frac{\partial(ru)}{\partial z}\right) \tag{2}$$

$$\frac{\partial(r\rho v)}{\partial t}+\frac{\partial(r\rho vv)}{\partial r}+\frac{\partial(r\rho vu)}{\partial z}=-r\frac{\partial P}{\partial r}+r\frac{\partial}{\partial r}\left(\frac{1}{\mathrm{Re}^*}\frac{1}{r}\frac{\partial(rv)}{\partial r}\right)+\frac{\partial}{\partial z}\left(\frac{1}{\mathrm{Re}^*}\frac{\partial(rv)}{\partial z}\right)+\rho ww \tag{3}$$

$$\frac{\partial(r^2\rho w)}{\partial t}+\frac{\partial(r^2\rho wv)}{\partial r}+\frac{\partial(r^2\rho ww)}{\partial z}=r^4\frac{\partial}{\partial r}\left(\frac{1}{\mathrm{Re}^*}\frac{1}{r}\frac{\partial(rw)}{\partial r}\right)+\frac{\partial}{\partial z}\left(\frac{1}{\mathrm{Re}^*}\frac{\partial(r^2w)}{\partial z}\right) \tag{4}$$

Here, u, v, and w are the axial, radial, and circumferential velocity components aligned with the z, r, and θ directions, respectively.

In Equations (1) through (4) the variable 1/Re* is defined as a combination of the liquid and gas Reynolds numbers which is a result of the two-phase treatment. The viscosity of a mixture can be written:

$$\mu = \alpha\mu_g + (1-\alpha)\mu_l \tag{5}$$

where α is the void fraction and μ_g and μ_l are the gas and liquid viscosities, respectively.[2] The pseudo-density is simply a statement about the amount of liquid mass in a cell and, therefore, can be related to the void fraction as shown in Equation (6).

$$\alpha = (\rho - 1)/(\rho_g/\rho_l - 1) \tag{6}$$

For cases where the density ratio is large, Equation (5) can be written as

$$\mu = (1-\rho)\mu_g + \rho\mu_l \tag{7}$$

Using Equation (7) when the Navier-Stokes equations are non-dimensionalized the definition for 1/Re* is found to be

$$\frac{1}{\mathrm{Re}^*} = \frac{\rho}{\mathrm{Re}_l} + \frac{(1-\rho)}{\mathrm{Re}_g}\left(\frac{\rho_g}{\rho_l}\right) \tag{8}$$

where ρ is the pseudo-density, ρ_g is the gas density, ρ_l is the liquid density, and Re_g and Re_l are the gas and liquid Reynolds numbers, respectively. The gas and liquid Reynolds numbers are defined:

$$\mathrm{Re}_g = \frac{\rho_g V_o D_o}{\mu_g} \tag{9}$$

$$\mathrm{Re}_l = \frac{\rho_l V_o D_o}{\mu_l} \tag{10}$$

In Equations (9) and (10), V_o and D_o are the gas axial inlet velocity and the radius of the gas core.

Finally, a constitutive relation for the pseudo-density is required for a well posed problem. For this case, the constitutive relation is simply that the material derivative is zero, since under the incompressible assumption the droplets move along a streamline undeformed. Surface tension forces are ignored in this treatment; in the high Weber number flow of interest, this permits resolution of mixing via computation of the local density as it evolves using the flux of liquid into and out of a given computational cell.

RESULTS AND DISCUSSION

The axisymmetric, unsteady, two-phase model has been validated through grid function convergence tests and analytic solutions for single phase flows. In addition, a multiblock grid, has been developed and optimized to resolve the waves formed on the liquid film in the important region just downstream of the collar. Results have been generated for the baseline geometry of experimental hardware to be tested in the near future at Purdue University. Parametric studies have been initiated to investigate the influence of various flow and design variables on the unsteady massflow and mixing characteristics delivered by the device. Nearly all solutions obtained show a quasi-periodic behavior due

to the formation of waves via the Kelvin-Helmholtz instability mechanism at the gas/liquid interface. It should be emphasized that at this point completely steady inflow conditions are assumed; the unsteadiness in the solution is an artifact of the hydrodynamic instability of the film – termed "self pulsation" by Dr. Bazarov and others.[3]

For the baseline case, the axial, radial, and azimuthal inlet velocities for the gas are 595 ft/s, 0, and 0, respectively. Additionally, the liquid inlet axial, radial, and azimuthal velocities are 95 ft/s, 0, and 179 ft/s. Furthermore, the gas core radius was 0.337 in., while the total length of the injector was 4.35 inches. Moreover, the mixing length, collar thickness and liquid film thickness was 0.68 in., 0.02in., and 0.0384 in., respectively. Finally, the gas Reynolds number, liquid Reynolds number, and density ratio are 3.9×10^6, 1.04×10^6, and 0.123, respectively.

Density contours for the region after the liquid injection and near the outer wall are plotted at several different times in Figure 2. The gas core is indicated by the lower dark black region, while the liquid film is upper light gray area in each image. A mixture of liquid and gas, indicated by a pseudo-density less than 1 but higher than the density ratio, is represented by intermediate colors. The presence of waves on the liquid surface is evident from Figure 2. As can be seen, the film oscillates with relatively uniform amplitude and frequency. The exit massflow rate, therefore, produced by the injector also oscillates at a fixed amplitude and frequency during "steady" operation, as the left plot in Figure 3 shows. For the baseline case, the variation in massflow rate, measured as the percent oscillation from the mean massflow rate, is 11.5 %. Obviously, the exit massflow rate is a maximum when a crest of a wave exits the injector and a minimum when the trough of a wave exits the injector.

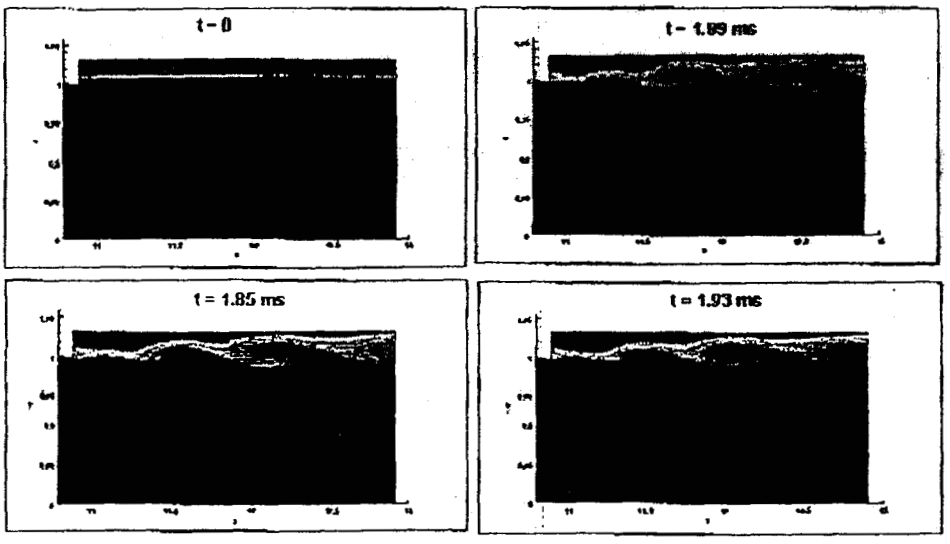

Figure 2. Contour plot of pseudo-density showing the presence of surface waves

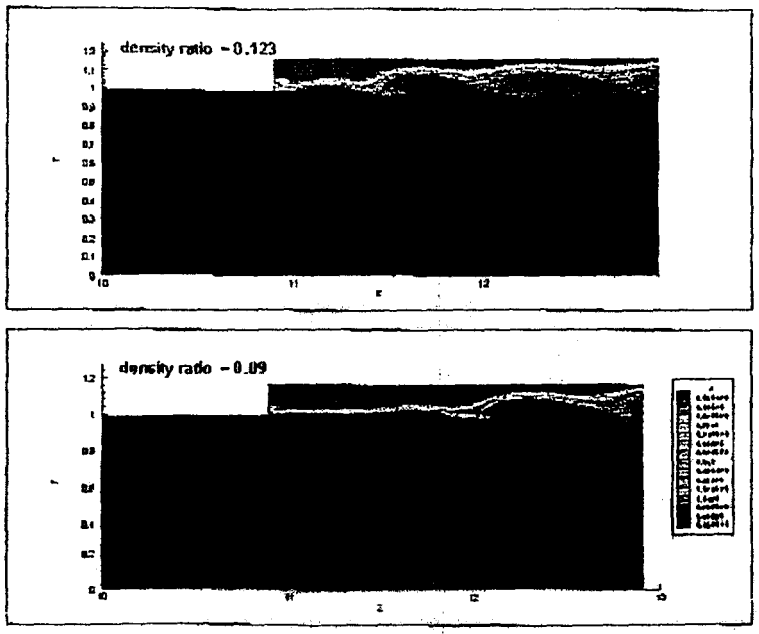

Figure 5. Comparison of the liquid film for density ratios of 0.09 and 0.0123

The effect of varying liquid swirl velocity was investigated in the second parametric study. In the following figures the liquid swirl velocity is presented as some fraction of the gas inlet velocity. For the baseline injector the liquid swirl velocity is 178 ft/s, which is 0.30 of the gas inlet axial velocity of 595 ft/s. Figure 6 shows that as the swirl velocity is increased the frequency of oscillation of the exit massflow rate decreases, until a swirl velocity of 0.45 is reached at which point the exit massflow rate does not vary. The trend is observed for two different density ratios of 0.09 and 0.123. As the swirl velocity increases, furthermore, the percent variation in the massflow rate increases. Again, this trend is only observed until a liquid swirl/gas velocity ratio of 0.45, at which point the film does not oscillate and the exit massflow rate is constant.

It seems natural to assume that as the swirl velocity increases the film would become more stable, since the film is forced against the outer wall by the increase in the azimuthal momentum. Therefore, the frequency of oscillation should decrease as the swirl velocity increases. However, it seams unusual that the percent variation in the exit massflow rate increases with increases in the swirl velocity. If the liquid film is visualized, as done in Figure 7, it can be seen that as the swirl velocity increases the liquid film begins to oscillate closer to the exit of the injector. As a result, less mixing is occurring in the injector as the swirl velocity is increased so larger variations in the exit massflow rate are observed.

The next parametric study was done by varying the initial thickness of the liquid film. The film thickness is reported as a nondimensional fraction of the gas core diameter. In this study the axial velocity of the liquid film was kept constant, in order to preserve the relative velocity difference between the gas and liquid. As a result, however, more liquid is being added as the initial thickness of the liquid is increased.

Figure 8 shows that as the initial liquid film thickness is increased, the frequency of oscillation of the film decreases slightly. Furthermore, the variation in the exit massflow rate doubles. Of course more massive objects tend to oscillate at lower frequencies, so the decrease in frequency as the film thickness increases seems natural. Moreover, as the film thickness increases, the liquid can support larger surface waves, thereby leading to an increase in the variation of the exit massflow rate. In Figure 9, the largest

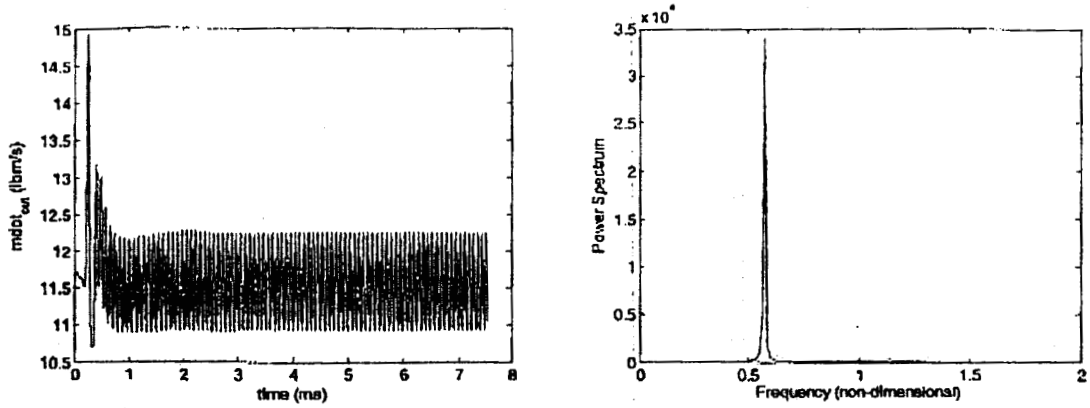

Figure 3. Exit massflow and Fast Fourier Transform of the exit massflow for the baseline case

The right plot in Figure 3 also shows a Fast Fourier Transform (FFT) of the exit massflow rate. Since the massflow rate at the exit oscillates at a uniform frequency for this case, a sharp peak in the FFT is evident at a nondimensional frequency of 0.572. The nondimensional frequency can by divided by the gas core radius and multiplied by the inlet gas velocity to yield a dimensional frequency of 12.1 kHz. This frequency is generally well above the critical chamber acoustic modes; oscillations of this nature are believed to affect the overall noise level produced by the engine, but probably to not play significant roles in acoustic instabilities.

In order to better understand how these types of coaxial swirl injectors behave, several parametric studies were performed. Since the most important dynamic information from the computations is the unsteady exit massflow rate produced by the injector, the amplitude and frequency of the oscillation will be presented from the parametric studies.

The first parametric study is the density ratio (gas/liquid), which was varied over a range of 0.09 to 0.20. Figure 4 shows that as the density ratio increases the frequency of the oscillation in the massflow rate increases. Since the gas momentum increases with density ratio, a larger force is exerted by the gas on the liquid surface leading to the increase in the observed frequency of oscillation. A similar result was obtained in prior work done on coaxial liquid centered injectors.[1]

Figure 4 illustrates that as the density ratio increases the variation of the massflow rate oscillations decreases. Initially, this result seems counterintuitive until the liquid film is visualized. As Figure 5 shows, the film begins to oscillate at a point farther down stream for the case where the density ratio is 0.09, therefore, less mixing between the gas and liquid has occurred. Consequently, the larger variation in massflow rate may be attributed to the decrease in mixing between cases.

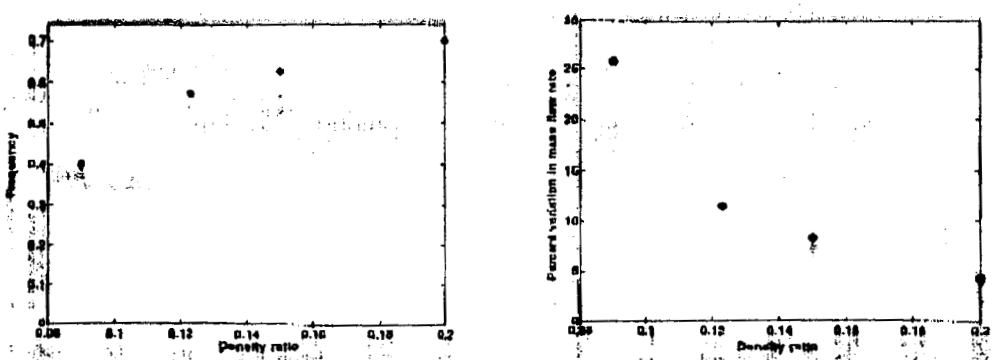

Figure 4. Frequency and variation of exit massflow rate oscillation for various density ratios

amplitude waves can be seen when the film thickness is 0.2, while the smallest amplitude waves occur when the film thickness is 0.07125.

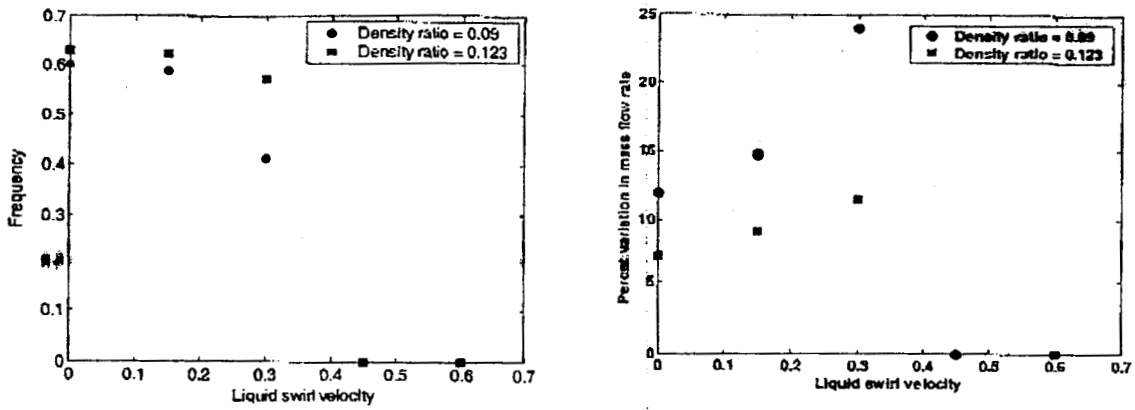

Figure 6. Frequency and variation of massflow rate oscillation for various liquid swirl velocities with density ratio as a parameter

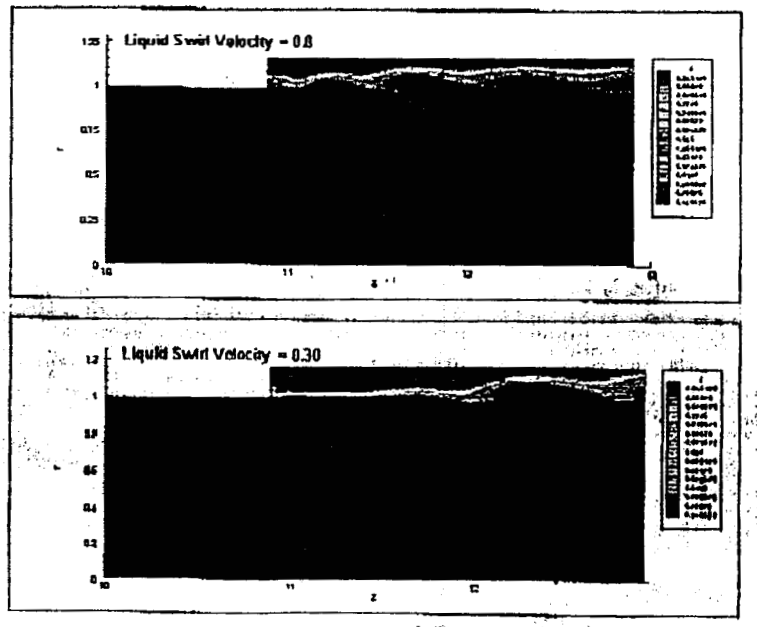

Figure 7. Visualization of the liquid film for a liquid swirl velocity of 0 and 0.3

The fourth parametric study is on the effect of the collar thickness on the dynamics performance of the injector. As Figure 10 shows there seems to be a minimum collar thickness below which the film does not oscillate. Due to this observation, it is hypothesized that the collar, acting as an aft facing step, plays a critical role in initiating film instability because of vortex shedding and reattachment.

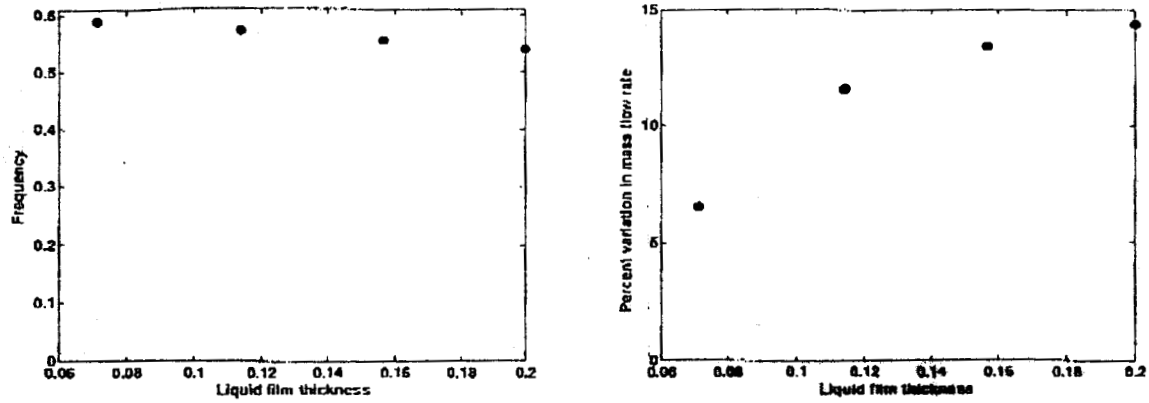

Figure 8. Frequency and variation of massflow rate oscillation for several liquid film thicknesses

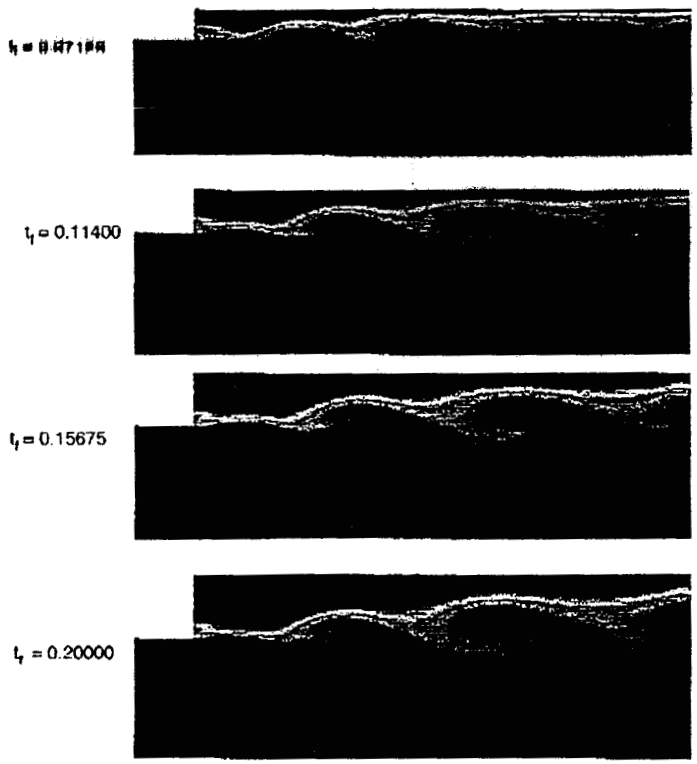

Figure 9. Liquid film visualization for film thickness study

The final parametric study is the effect of mixing length on the film behavior. It is interesting to note from Figure 11 that the frequency of oscillation of the liquid film is independent of the mixing length. This result seems natural, since the frequency of oscillation should be dependent on the vortex shedding from the collar and the imbalance of dynamic pressure on the liquid surface. The mixing length does not affect either one of these quantities, so the frequency of oscillation should be independent of mixing length.

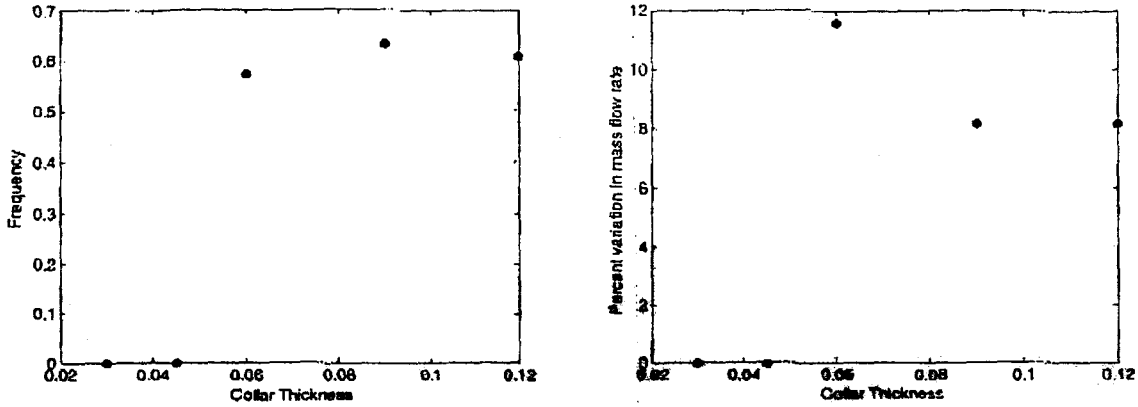

Figure 10. Frequency and variation of massflow rate oscillation as a function of collar thicknesses

Figure 11 also demonstrates that in general the variation in the mass flow rate decreases with an increase in the mixing length. It is expected that increasing the mixing length would allow the liquid and gas to mix further, thereby reducing the amplitude of the surface waves before exiting the injector. While Figure 11 does show this trend, there are points that are local minima and maxima. However, the percent variation in the mass flow rate is actually a measure of temporal variation of the massflow rate. Therefore, the time averaged value of the exit liquid film thickness, defined by where the pseudo-density is larger than 0.95, was computed. Figure 12 is a plot of the time averaged exit film thickness and shows that indeed the value does decrease monotonically as the mixing length increases.

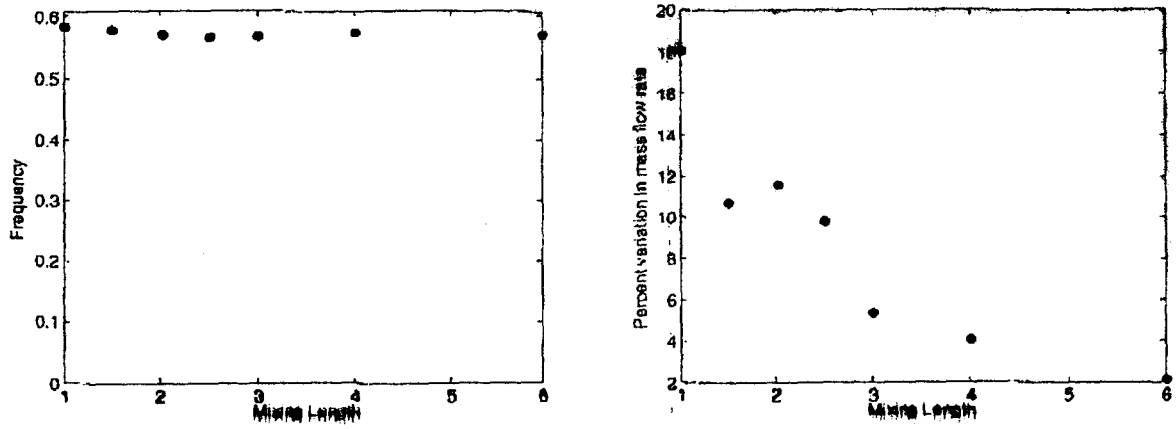

Figure 11. Frequency and variation of massflow rate oscillation as a function of the mixing length

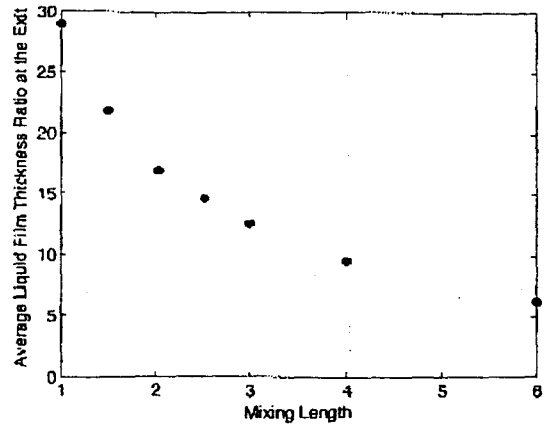

Figure 12. Time average liquid film thickness at the exit of the injector as a function of mixing length

Figure 13 offers further proof that the local minima and maxima observed in Figure 11 is a function of how the variation in massflow rate is defined. As Figure 13 shows, the surface waves near the exit of the injector become less pronounced as the mixing length increases. This indicates that as the mixing length increases the amount of mixing that occurs in the injector also increases. It is also important to remember that some liquid film needs to be present at the exit of the injector to provide adequate cooling for the injector face. Therefore, an optimal mixing length exists which provides the required mixing while leaving a thick enough film at the exit to provide cooling.

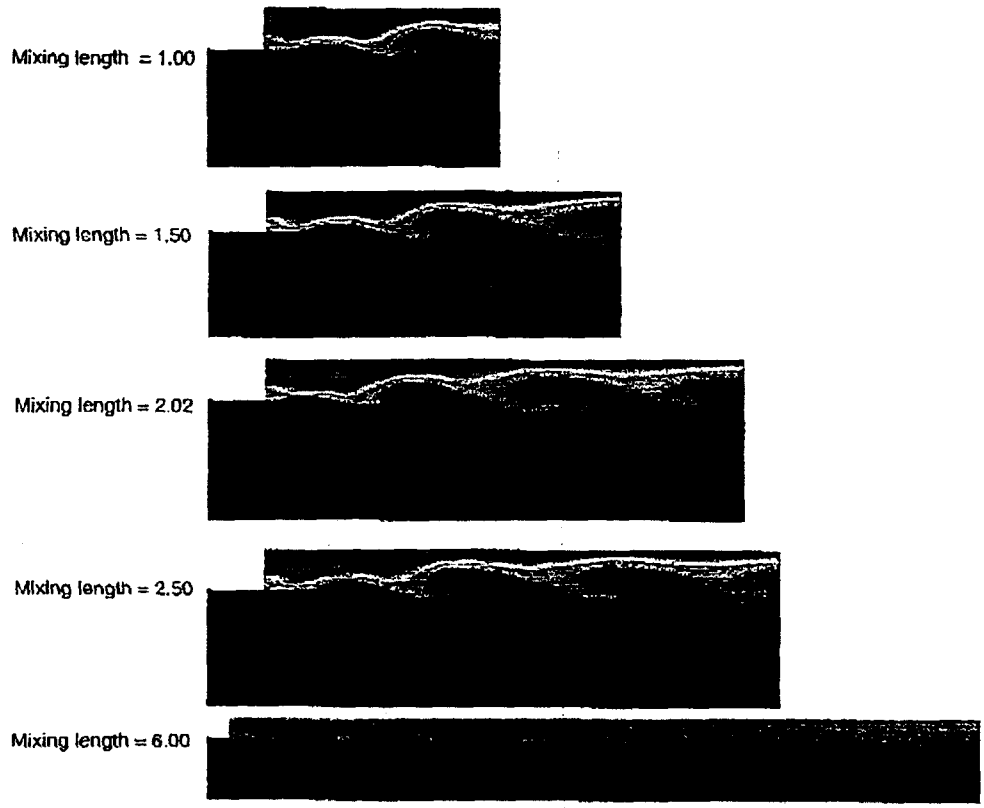

Figure 13. Visualization of the liquid film for various mixing lengths

SUMMARY AND CONCLUSIONS

The unsteady, axisymmetric, swirling flow numerical model for the laminar Navier-Stokes equations for this two-phase flow is capable of assessing the time-dependent orifice exit conditions for arbitrary fuel and oxidizer gas injection conditions. Parametric studies have been conducted to determine the effect of density ratio, liquid swirl velocity, film thickness, collar thickness, and mixing length. It has been found that the frequency at which the liquid film oscillates increases as the density ratio and collar thickness increase, decreases as the film thickness and liquid swirl velocity increase, and is unaffected by the mixing length. It is believed that the frequency is dependent on the behavior of the vortex shedding/reattachment from the collar and the dynamics pressure imbalance on the liquid surface. The fact that the collar thickness affects the frequency leads to the inclusion of the vortex behavior as an important parameter on the behavior of the film.

Additionally, the variation in the massflow rate increases as the liquid swirl velocity and liquid film thickness increase and decreases as the mixing length and density ratio increase. The variation in massflow rate increases with swirl velocity because mixing is inhibited, so larger amplitude waves reach the exit of the injector. The variation in massflow rate increases with liquid film thickness since larger amplitude waves can be supported by thicker liquid films. As the mixing length increases, moreover, the variation in the massflow rate tends to decrease. However, it was found that the time averaged film thickness at the exit does monotonically decrease as the mixing length increase. Furthermore, the massflow rate is inversely related to density ratio since the film starts to oscillate closer to the edge of the collar at larger density ratios. This means that the surface waves have a longer effective mixing length at higher density ratios leading to a decrease in the variation in massflow rate.

ACKNOWLEDGMENTS

This work was accomplished under NASA Space Act Agreement NCC8-200. Our team thanks Brent Harper the COTR, and Garry Lyles and his staff for their technical inputs and encouragement.

REFERENCES

1. Kim, B-D, and Heister, S. D., "Two-Phase Modeling of Hydrodynamic Instabilities in Coaxial Injectors," to appear, *J. Propulsion and Power*, 2004.

2. Akihiro Kubota et al., "A New Modeling of Cavitating Flows: A Numerical Study of Unsteady Cavitation on a Hydrofoil Section", *Journal of Fluid Mechanics*, Vol. 240, pp. 59-96, 1992.

3. Bazarov, V., "Self-Pulsations in Coaxial Injectors with Central Swirl Liquid Stage", AIAA 95-2358, *31st AIAA/ASME/ASE/ASEE Joint Propulsion Conference and Exhibit*, San Diego, CA.